NANO LETTERS

2006
Vol. 6, No. 10
2232−2237

Electrokinetic Energy Conversion Efficiency in Nanofluidic Channels

Frank H. J. van der Heyden, Douwe Jan Bonthuis, Derek Stein, Christine Meyer, and Cees Dekker*

Kavli Institute of Nanoscience, Delft University of Technology, Lorentzweg 1, 2628 CJ Delft, The Netherlands

Received July 3, 2006; Revised Manuscript Received August 7, 2006

ABSTRACT

We theoretically evaluate the prospect of using electrokinetic phenomena to convert hydrostatic energy to electrical power. An expression is derived for the energy conversion efficiency of a two-terminal fluidic device in terms of its linear electrokinetic response properties. For a slitlike nanochannel of constant surface charge density, we predict that the maximum energy conversion efficiency occurs at low salt concentrations. An analytic expression for the regime of strong double-layer overlap reveals that the efficiency depends only on the ratio of the channel height to the Gouy–Chapman length, and the product of the viscosity and the counterion mobility. We estimate that an electrokinetic energy conversion device could achieve a maximum efficiency of 12% for simple monovalent ions in aqueous solution.

A pressure-driven fluid flow through a narrow channel carries a net electrical charge with it, inducing both a current and a potential when the charge accumulates at the channel ends. These so-called streaming currents and streaming potentials can drive an external load and therefore represent a means of converting hydrostatic energy into electrical power. The notion of employing such electrokinetic effects in an energy conversion device is not new,[1] yet has received renewed attention in the context of micro- and nanofluidic devices[2−5] whose geometries and material properties can be engineered. High energy-conversion efficiency and high output power are the requirements for such a device to be practical. Physical modeling of electrokinetic energy conversion is needed to guide the optimization of these properties.

Electrokinetic phenomena originate from a combination of two microscopic causes, illustrated in Figure 1a: (i) viscous forces couple the motion of dissolved ions to that of the surrounding fluid and (ii) charged channel surfaces induce the accumulation of counterions into a screening layer of net opposite charge, called the double layer. It is conventional to model the distribution of electrostatic charge near a charged boundary using the Poisson−Boltzmann description of an electrolyte and to couple its transport to that of the fluid using the Navier−Stokes equation. This theoretical framework has been used by several authors to calculate the theoretical energy conversion efficiency of fluidic devices, yielding maximum efficiencies ranging from ∼0.1% to ∼1%.[1−4] These calculations applied approximations that are valid only for the case of low electrostatic potentials and nonoverlapping double layers and assign a constant potential, called the ζ potential, to parametrize the

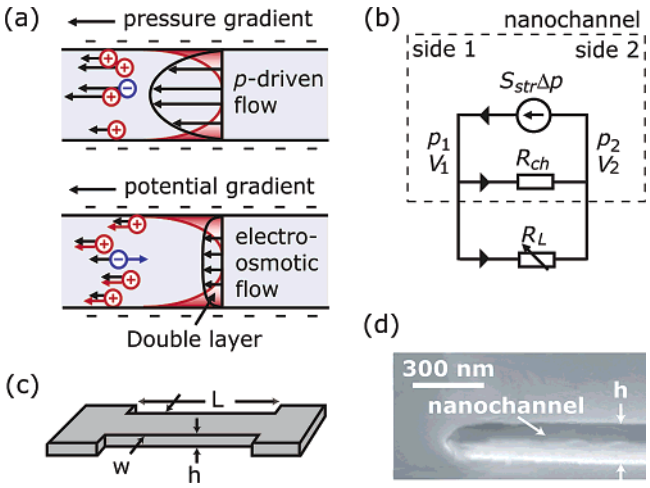

Figure 1. (a) Schematic illustration of electrokinetic effects. Top: a pressure-driven flow carries ionic charge within the double layer, generating a streaming current. Bottom: the electric field-driven transport of ions results in an electro-osmotic flow. The velocity of individual ions consists of a fluid-driven (black arrows) and an electric-field-driven part (colored arrows). (b) Equivalent electronic circuit of a nanochannel (dashed box) connected to a load resistor. We define $\Delta p = p_2 - p_1$, $\Delta V = V_2 - V_1$, and all ionic and liquid flows in the direction from side 2 to side 1. The arrows indicate the ionic current directions for a positive applied Δp during power generation. (c) Schematic 3D nanochannel geometry used in our calculations. (d) Side view of a ∼200-nm-high silica nanochannel, imaged by scanning electron microscopy.

electrostatic condition of the surface. Recent investigations of ionic transport and streaming currents in well-defined, nanoscale fluidic channels have demonstrated how electrokinetic phenomena can be understood in the regimes of high surface potentials and overlapping double layers.[5−8] In these

* Corresponding author. E-mail: dekker@mb.tn.tudelft.nl.

10.1021/nl061524l CCC: $33.50
Published on Web 09/16/2006

regimes, the full, nonlinear Poisson−Boltzmann description of the electrolyte is needed. It was also confirmed that a constant ζ potential boundary condition is a poor description of the silica surface under different salt and pH conditions and that a constant or chemically reactive surface charge density is more appropriate.[6,7]

In this paper, we present a theoretical analysis of electrokinetic energy conversion efficiency. We first provide an expression for the efficiency in terms of the measurable linear electrokinetic responses of any two-terminal fluidic device. We then calculate the efficiency for a particular geometry, namely, a rectangular, slitlike channel, using the full Poisson−Boltzmann description of the electrolyte which includes the effects of double-layer overlap, and a constant surface charge density as an appropriate description of the surface. In contrast to previous work that used a constant ζ potential as a boundary condition, our model predicts the highest efficiency for low salt concentrations in nanoscale fluidic channels, where electric double layers overlap. An analytical expression for the efficiency in this important regime is presented. It reveals that the optimal efficiency results at a surface charge density that balances the tradeoffs between the increased charge transport and the increased electrical power dissipation that occur at high surface charge densities. We predict that channels can be optimized to deliver 12% energy conversion efficiency using aqueous solutions with common ions.

Energy Conversion Efficiency of a Fluidic Device of Arbitrary Geometry and Surface Charge. The electrokinetic properties of a fluidic device can be characterized experimentally by the response of the ionic current, I, and the fluid volume flow rate, Q, to either an applied pressure difference, Δp, or an applied electrochemical potential difference, ΔV, across the device. We are interested in calculating the energy conversion efficiency in the linear response regime, where I and Q can be described by

$$I = \frac{\mathrm{d}I}{\mathrm{d}\Delta p}\Delta p + \frac{\mathrm{d}I}{\mathrm{d}\Delta V}\Delta V \equiv S_{\mathrm{str}}\Delta p + \frac{\Delta V}{R_{\mathrm{ch}}} \tag{1}$$

$$Q = \frac{\mathrm{d}Q}{\mathrm{d}\Delta p}\Delta p + \frac{\mathrm{d}Q}{\mathrm{d}\Delta V}\Delta V \equiv \frac{\Delta p}{Z_{\mathrm{ch}}} + S_{\mathrm{str}}\Delta V \tag{2}$$

which define the constants: R_{ch}, the electrical resistance of the channel; Z_{ch}, the fluidic impedance of the channel; and S_{str}, the streaming conductance.[6] Linear electrokinetic behavior is expected as long as the electrostatic double layers are not significantly distorted by the fluid flows or by the applied electrostatic potentials.[9] Note that we have made use of the Onsager relation $\mathrm{d}Q/\mathrm{d}\Delta V = \mathrm{d}I/\mathrm{d}\Delta p \equiv S_{\mathrm{str}}$, which is an expression of the reciprocity between electrically induced fluid flows, and flow-induced electrical currents.[9−11]

The ability of such a fluidic device to translate hydrostatic energy into electrical power, driven through a load resistance, R_{L}, can be calculated by analyzing the equivalent circuit presented in Figure 1b. Under an applied pressure difference, Δp, the output streaming potential reaches an equilibrium value, $\Delta V = -S_{\mathrm{str}}\Delta p(R_{\mathrm{ch}}R_{\mathrm{L}})/(R_{\mathrm{ch}} + R_{\mathrm{L}})$, from which the output power, $\Delta V^2/R_{\mathrm{L}}$, is determined. The ratio of the output power to the input pumping power, $Q\Delta p$, is the electrokinetic energy conversion efficiency, ε. It is convenient to define a dimensionless parameter, α, that provides a relative measure for the coupling between electrical and fluid transport

$$\alpha \equiv S_{\mathrm{str}}^2 Z_{\mathrm{ch}} R_{\mathrm{ch}} \tag{3}$$

and a rescaled load resistance, Θ, relative to the channel resistance

$$\Theta \equiv \frac{R_{\mathrm{L}}}{R_{\mathrm{ch}}} \tag{4}$$

In terms of these device characteristics, the electrokinetic energy conversion efficiency is given by

$$\varepsilon = \frac{\alpha\Theta}{(1+\Theta)(1+\Theta-\alpha\Theta)} \tag{5}$$

The maximum efficiency, $\varepsilon_{\mathrm{max}}$, achieved at a load resistance of $\Theta = 1/\sqrt{1-\alpha}$, is found to be

$$\varepsilon_{\mathrm{max}} = \frac{\alpha}{\alpha + 2\left(\sqrt{1-\alpha}+1-\alpha\right)} \tag{6}$$

$\varepsilon_{\mathrm{max}}$ increases from 0% at $\alpha = 0$ toward the limit of 100% as α approaches 1, while conservation of energy requires that $\alpha \leq 1$. Interestingly, optimal energy conversion efficiency is achieved for $R_{\mathrm{L}} > R_{\mathrm{ch}}$. By matching channel and load impedance, that is, $R_{\mathrm{L}} = R_{\mathrm{ch}}$, the system is instead optimized to deliver the maximum power for a given Δp.

Because of the reciprocity between eqs 1 and 2, this theory works equally well for describing the efficiency by which electrical energy is converted into fluid pumping power, an effect that is known as electro-osmotic pumping (Figure 1a).[12,13] By considering the pumping power of the electrokinetic device through a fluidic load impedance, Z_{L}, a similar analysis determines the pumping efficiency to be the ratio of the output pumping power, $\Delta p^2/Z_{\mathrm{L}}$, to the input electrical power, $I\Delta V$. By redefining $\Theta \equiv Z_{\mathrm{L}}/Z_{\mathrm{ch}}$, eqs 5 and 6 are made to describe the efficiency of electro-osmotic pumping.

Calculations of the Energy Conversion Efficiency in a Slitlike Nanochannel. The electrokinetic behavior of a fluidic device derives from its physical geometry, surface properties, and from the properties of the fluid filling it. In this section, we calculate the electrokinetic energy conversion efficiency of a long, rectangular, slitlike fluidic nanochannel, whose channel walls are uniformly charged, and whose length L, width w, and height h satisfy $L \gg h$ and $w \gg h$ so that we can ignore end effects and treat the system as infinite parallel plates (Figure 1c and d). The channel is filled with aqueous solution of viscosity, η, and monovalent salt concentration, n. This particular system is chosen for several reasons: (i) numerical calculations of electro-osmotic pumping indicated that the parallel-plate geometry has the highest

efficiency;[13] (ii) the potential and charge distributions, described by Poisson-Boltmann theory, and the fluid velocity, described by a Poiseuille flow with no-slip boundary conditions, have exact solutions; and (iii) rectangular channels with high aspect ratios[6,7] and tunable microslits[14] have been used extensively to study electrokinetic effects.

The electrostatic potential, $(kT/e)\psi(x)$, at height x from the channel midplane is described by the mean-field Poisson−Boltzmann equation for a monovalent salt

$$\frac{d^2\psi}{dx^2} = \kappa^2 \sinh(\psi(x)) \tag{7}$$

where $\psi(x)$ is the dimensionless potential, e is the electron charge, kT is the thermal energy, $1/\kappa$ is the Debye screening length, defined by $\kappa^2 = 2e^2n/(\epsilon\epsilon_0 kT)$, and $\epsilon\epsilon_0$ is the permittivity of water. The analytical solution for $\psi(x)$ for a symmetrical channel can be expressed as[15,16]

$$\psi(x) = \psi(0) + 2\ln\left(\mathrm{JacCD}\left(\frac{\kappa x}{2} e^{-\psi(0)/2}\middle| e^{2\psi(0)}\right)\right) \tag{8}$$

where JacCD($z|m$) is the Jacobian elliptical function with argument z and parameter m. This exact solution of $\psi(x)$ includes the effects of double-layer overlap and defines the density of positive and negative ions, n_+ and n_-, through the Boltzmann equation: $n_\pm(x) = ne^{\mp\psi(x)}$. The net charge density, $\rho(x)$, is found using Poisson's equation, $\rho(x) = -(\epsilon\epsilon_0 kT/e)(\partial^2\psi(x)/\partial x^2)$.

The fluid flow induced by and contributing to the transport of ions is described by the Navier−Stokes equation

$$\eta\frac{d^2u(x)}{dx^2} - \frac{\Delta V}{L}\frac{\epsilon\epsilon_0 kT}{e}\frac{d^2\psi(x)}{dx^2} + \frac{\Delta p}{L} = 0 \tag{9}$$

where $u(x)$ is the fluid velocity at height x. A no-slip boundary condition is imposed at the channel walls, $x = \pm h/2$. Solving eq 9 for $\Delta V = 0$ or $\Delta p = 0$ yield, respectively, the pressure-driven velocity profile $u_P(x) = (\Delta p/8\eta L)(h^2 - 4x^2)$ and the electro-osmotic velocity profile $u_V(x) = (\epsilon\epsilon_0\Delta V/\eta L)[(kT/e)\psi(x) - \zeta]$, where ζ is the potential at the no-slip plane.

Equations 7−9 form the basis for calculating Z_{ch}, R_{ch}, and S_{str}, which define the energy conversion efficiency through eqs 3−5 using the following expressions for a slitlike channel

$$\frac{1}{Z_{ch}} = \frac{w}{\Delta p}\int_{-h/2}^{h/2} u_P(x)\,dx = \frac{wh^3}{12\eta L} \tag{10}$$

$$\frac{1}{R_{ch}} = \frac{w}{\Delta V}\int_{-h/2}^{h/2}\left[\frac{\Delta V}{L}\sum_i e n_i(x)\mu_i + \rho(x)\,u_V(x)\right]dx \tag{11}$$

$$S_{str} = \frac{w}{\Delta p}\int_{-h/2}^{h/2}\rho(x)\,u_P(x)\,dx \tag{12}$$

where μ_i and n_i are the electrophoretic mobility and the density of ion species i, respectively. The fluidic impedance

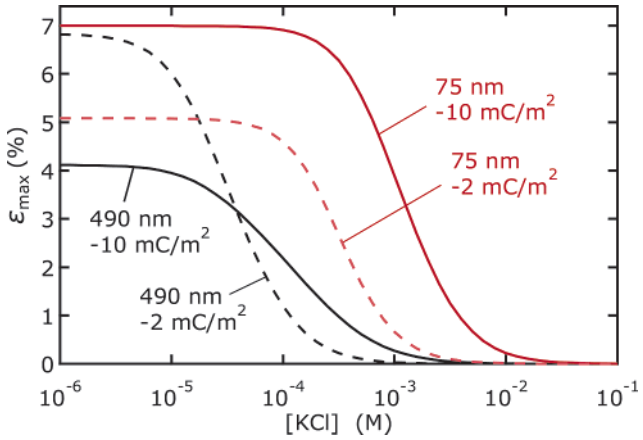

Figure 2. KCl concentration dependence of ε_{max} for channel heights $h = 75$ (red curves) and 490 nm (black curves) and surface charge densities $\sigma = -10$ (solid curves) and -2 mC/m^2 (dashed curves), calculated using the exact expressions of eqs 3−13 with the parameters specified in ref 18. These results account for both co- and counterions and include the effects of double-layer overlap.

(eq 10) is the familiar result for Poiseuille flow in a slitlike channel and should apply as long as the Navier−Stokes equation (eq 9) is valid.[17] The behavior of R_{ch} and S_{str} is nontrivial and has been investigated recently in silica nanochannels:[6,7] The electrical conductance (eq 11) consists of contributions from electrophoretic ion transport through the fluid and convective transport of charge. R_{ch} was found to exhibit a surface-charge-governed low-n plateau due to the transport of counterions in the double layer, and a decrease with increasing n in the high-n, bulk transport regime. These results for silica were best described by applying a constant surface charge density, σ, as a boundary condition.[7] The streaming conductance (eq 12) exhibits a low-n plateau in the double-layer-overlap regime, which is also captured by a constant-σ boundary condition, and a decay at high n, which was best modeled by a chemical equilibrium model of σ.[6]

These experiments on silica nanochannels indicate that a constant σ is a good description of the electrostatic condition of the channel walls at low salt, a fair approximation at high salt, and in all cases better than assuming a constant ζ. We therefore impose a constant surface charge density of the channel walls, which relates to $\psi(x)$ through Gauss' Law:

$$\sigma = \pm\frac{\epsilon\epsilon_0 kT}{e}\frac{d\psi(x)}{dx}\bigg|_{x=\pm h/2} \tag{13}$$

Equations 3−13 are exact and valid for all channel heights, including the regime of double-layer overlap. These equations were evaluated numerically using Maple to generate the plots in Figures 2 and 3: First, the potential distribution (eq 8) is calculated for a given channel height, salt concentration, and the boundary condition of a constant σ (eq 13). This potential is then used to calculate the electrokinetic response properties through eqs 10−12, from which α (eq 3) and ε_{max} (eq 6) are finally obtained.

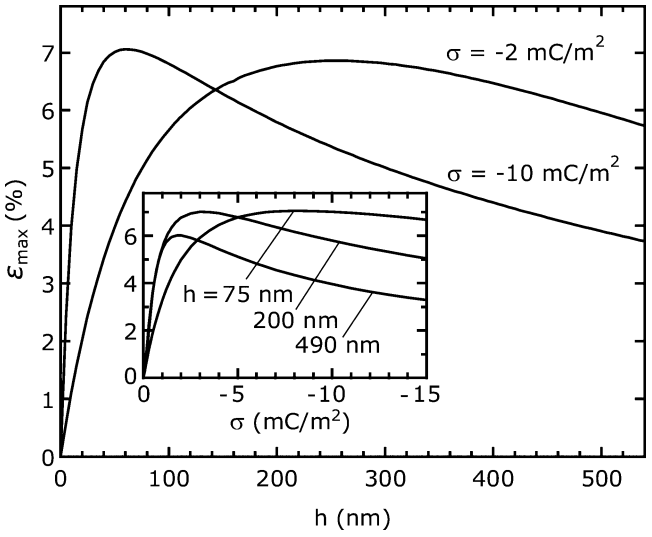

Figure 3. Channel height and surface charge density dependence of ε_{max}, calculated for 10^{-5} M KCl using the exact expressions of eqs 3−13, which include the effects of double-layer overlap. The main panel shows ε_{max} as function of h for high ($\sigma = -10$ mC/m^2) and low (−2 mC/m^2) surface charge densities. The inset plots ε_{max} as function of σ for the channel heights 75, 200 and 490 nm. Because n is only 10^{-5} M, the calculated ε_{max} in this figure is close to the low-n plateau values in Figure 2.

Figure 2 shows the calculated salt dependence of ε_{max} for channels filled with an aqueous solution of potassium chloride (KCl). For $h = 75$ nm and $h = 490$ nm channels with fixed surface charge densities, the highest ε_{max} occurs in a low-n plateau, followed by a decay to zero efficiency at high n. The plateau region extends to higher n for smaller channels: up to $n = 10^{-5}$ M for a $h = 490$ nm channel, and up to $n = 10^{-4}$ M for a $h = 75$ nm channel. The height of the plateau clearly depends on both h and σ, as can be seen by comparing the curves in Figure 2.

The high energy-conversion efficiency that occurs at low salt conditions can be understood intuitively: At sufficiently low n, where $\kappa h \ll 1$, electrostatic forces expel co-ions from the channel, leaving only counterions. Because co-ions do not add to the generated electrical power by streaming currents, but instead provide an additional pathway for power dissipation through ionic conductance, they can only detract from the energy conversion efficiency. The power and streaming current are both maximal for low n, where the current originates from the transport of counterions that are induced by the fixed surface charge.

Figure 3 shows ε_{max} as function of h and σ, calculated using eqs 3−13 for a low salt concentration of 10^{-5} M KCl, where the efficiency should be close to its low-n plateau value of Figure 2. ε_{max} is found to have a maximum as function of both h and σ (Figure 3). For fixed σ, ε_{max} increases quickly from zero at $h = 0$ nm to a peak of about 7% before decaying slowly with h, both for $\sigma = -2$ mC/m^2 and $\sigma = -10$ mC/m^2. The peak in ε_{max} shifts to higher h as σ decreases: It occurs at $h \simeq 250$ nm for $\sigma = -2$ mC/m^2, and at $h \simeq 60$ nm for $\sigma = -10$ mC/m^2. A similar behavior of ε_{max} is seen for fixed h and changing σ (inset): the peak efficiency shifts to higher σ when h decreases. The peak value of 7% barely depends on h for small channels. Only for higher h is the peak efficiency slightly reduced (to ∼6% for $h = 490$ nm).

Electrokinetic Energy Conversion in the Limit of Strong Double-Layer Overlap. The electrokinetic energy conversion efficiency peaks as a function of channel height and surface charge density in the low salt regime because of the competition between two opposing effects: As σ is raised, the increased counterion density results in an increased convective charge transport by a pressure-driven flow (enhancing power generation), while also providing a path for resistive power dissipation. The scaling of these effects with σ depends on the distribution of counterions across the fluid velocity profile, which determines the optimal surface charge density for a given channel height. This interplay, as well as the influence of ion mobility and fluid viscosity, is clearly revealed by an analytic approximation that we derive for the low salt limit: In the absence of co-ions, which occurs when $\kappa h \ll 1$, the analytic solution to the Poisson−Boltzmann equation (eq 7) simplifies to[16]

$$\psi(x) = 2\ln\left[\cos\left(\frac{Kx}{2}\right)\right] + \psi(0) \tag{14}$$

where the inverse length $K \equiv \kappa e^{-\psi(0)/2}$ contains an integration constant,[19] $\psi(0)$. The electrostatic potential distribution is fully specified by imposing the constant-surface-charge boundary condition (eq 13), which gives

$$\frac{Kh}{4}\tan\frac{Kh}{4} = \frac{h}{2\lambda} \tag{15}$$

The Gouy−Chapman length, $\lambda = 2\epsilon\epsilon_0 kT/(e|\sigma|)$, defines a layer within which most counterions are localized. By inserting eq 14 into the expressions for Z_{ch}, R_{ch}, and S_{str} (eqs 10−12), we obtain an analytical expression for α, as defined in eq 3

$$\alpha = \frac{3\left[\frac{4}{Kh}\int_0^{Kh/4} y\tan(y)\,dy\right]^2}{\frac{Kh}{4}\tan\frac{Kh}{4}\left(1+\frac{\mu\eta e}{2\epsilon\epsilon_0 kT}\right) - \left(\frac{Kh}{4}\right)^2} \tag{16}$$

from which the maximum efficiency (eq 6) can be calculated directly. The efficiency in the regime of strong double-layer overlap, when solved for the case of a constant surface charge density (eq 15), only depends on the following two dimensionless parameters: (i) $\mu\eta e/2\epsilon\epsilon_0 kT$, which contains the fluid and ion properties η and μ, and (ii) $h/2\lambda$, which explains the reciprocal behavior of h and σ observed in Figure 3.

The competing effects of ionic and streaming conductance result in a peak value of ε_{max} at $h/2\lambda \approx 8$, or equivalently at $h|\sigma| \approx 0.6$ nm × C/m^2, as can be seen from the solid lines in Figure 4. Calculations of ε_{max} using eqs 3−13 with Cl^- as the co-ion, $n = 10^{-5}$ M, and a fixed $\sigma = -10$ mC/m^2 yield curves that are indistinguishable from these solid lines, demonstrating the validity and accuracy of eq 16 for low but realistic salt concentrations. Because the highest ε_{max}

occurs for a relatively high surface charge, that is, $h/2\lambda \gg 1$, we can estimate K in the high-σ limit, $h/2\lambda \rightarrow \infty$, which implies $Kh/4 \rightarrow \pi/2$ from eq 15. Expanding eq 15 in a Laurent series around $Kh = 2\pi$ gives

$$K \simeq \frac{2\pi}{2\lambda + h} + \mathcal{O}\left(\frac{Kh}{4} - \frac{\pi}{2}\right) \tag{17}$$

This high-σ approximation for $\psi(x)$ in the absence of co-ions leads, through eqs 11 and 12, to the following approximations of the ionic resistance and the streaming conductance

$$\frac{1}{R_{ch}} \simeq \frac{w}{L\eta}\left(\frac{2\epsilon\epsilon_0 kT}{e}\right)^2\left(1 + \frac{\mu\eta e}{2\epsilon\epsilon_0 kT}\right)\frac{2}{\lambda} \tag{18}$$

$$S_{str} \simeq \frac{w}{L\eta}\frac{2\epsilon\epsilon_0 kT}{e}h\left[\left(\frac{2\lambda}{h} + 1\right)\ln\left(1 + \frac{h}{2\lambda}\right) - 1\right] \tag{19}$$

The ionic conductance, which dissipates power, is proportional to the surface charge density (eq 18) because $|\sigma| \propto 1/\lambda$, whereas S_{str}, which is responsible for electrical power generation, increases linearly for small $|\sigma|$, and logarithmically as function of large $|\sigma|$ (eq 19). R_{ch} and S_{str} are used to approximate the electrokinetic energy conversion efficiency through eqs 3 and 6, yielding

$$\varepsilon_{max} \simeq \frac{3}{4}\frac{\frac{2\lambda}{h}\left[\left(\frac{2\lambda}{h} + 1\right)\ln\left(1 + \frac{h}{2\lambda}\right) - 1\right]^2}{1 + \frac{\mu\eta e}{2\epsilon\epsilon_0 kT}} + \mathcal{O}\left[\left(\frac{2\lambda}{h}\right)^2\right] \tag{20}$$

This simple expression for the efficiency captures the most important features of the exact solution, as seen in the comparison presented in Figure 4: (i) ε_{max} increases linearly for small $h/2\lambda$, peaks at $h/2\lambda \approx 8$, and finally decreases at higher $h/2\lambda$ and (ii) the efficiency is higher for counterions with a lower mobility.

The shape of ε_{max} as function of $h/2\lambda$ is explained by the gradual shift from a homogeneous counterion distribution for small surface charge densities to a strong counterion accumulation close to the surface for high surface charge densities. In the low-salt regime (no co-ions), the number of counterions in the nanochannel is proportional to the surface charge density due to the imposed charge neutrality, which explains the linear relation, $1/R_{ch} \propto |\sigma|$, from eq 18. When these counterions are distributed homogeneously across the channel, they probe the fluid velocity profile evenly, which yields the same proportional scaling for the streaming conductance, $S_{str} \propto |\sigma|$. The linear increase of ε_{max} with surface charge in the low-σ limit then follows from $\varepsilon_{max} \propto R_{ch}S_{str}^2$ (see ref 21). For high surface charge densities, the counterions become localized very close to the charged channel walls where they barely contribute to the streaming conductance because of the low fluid speed there. In this limit of very high σ, ε_{max} becomes dominated by the channel resistance, which decreases as $1/|\sigma|$.

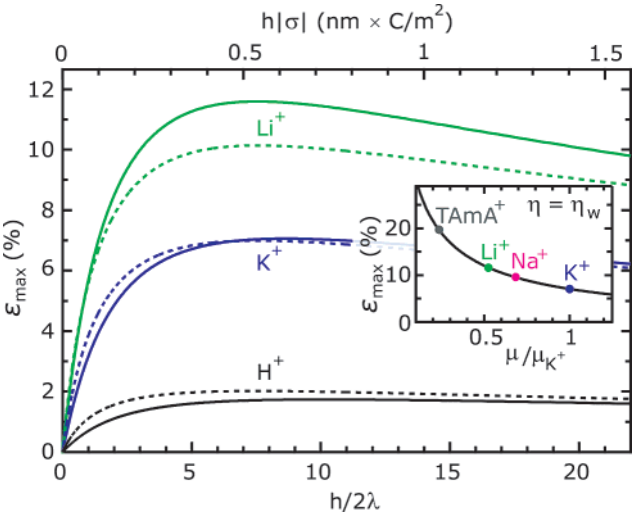

Figure 4. Calculated ε_{max} dependence on the degree of Gouy−Chapman-layer overlap in the low salt limit (no co-ions) for three counterion types. The solid lines represent the exact solution of eq 16, and the dashed lines represent the approximation of eq 20. Calculations using eqs 3−13 with Cl^- as the co-ion, a low salt concentration of $n = 10^{-5}$ M, and a fixed $\sigma = -10$ mC/m^2 yield curves that are indistinguishable from the solid lines. The bottom axis shows the $h/2\lambda$ dependence, and the top axis shows the equivalent $h|\sigma|$ dependence. Inset: the peak value ε_{max} as function of the counterion mobility relative to the case of potassium ions ($\mu = \mu_{K^+}$) in water ($\eta = \eta_w$). The circles indicate ions of different mobility in aqueous solution. The values of the physical parameters used in the calculations appear in ref 18. The same curve for ε_{max} is obtained when plotted against the renormalized viscosity, η/η_w with constant $\mu = \mu_{K^+}$.[20]

The efficiency increases with decreasing ion mobility (Figure 4) because ionic conductance leads to power dissipation. Peak efficiency values of 2%, 7%, and 12% are obtained for aqueous solutions containing H^+, K^+, and Li^+, respectively. This maximal efficiency, found by solving $\partial\varepsilon_{max}/\partial(h/2\lambda) = 0$, depends only on the remaining parameter,[22] $\mu\eta e/2\epsilon\epsilon_0 kT$ and is plotted as function of the rescaled ion mobility for aqueous solution in the inset of Figure 4. Because the mobility of Li^+ is the lowest among simple monovalent ions, 12% represents the upper limit of the electrokinetic energy conversion efficiency predicted for an aqueous system with common ions. This efficiency can be further improved to around 20% using more complex monovalent ions such as tetra-*n*-amylammonium$^+$ ($TAmA^+$).

The preceding calculations of electrokinetic power generation and efficiency neglect the possible effects of "Stern conductance".[23] This electrical conductance is invoked to explain the differences that are often seen between the electrical surface properties inferred from different types of electrokinetic measurements and is assumed to occur in the Stern layer, the first molecular layers directly adjacent to a hard surface where liquid and ion properties may differ from the bulk values and where mean-field Poisson−Boltzmann theory breaks down. The conventional microscopic picture of Stern conductance is that ions in the Stern layer are mobile in response to an electric field but not to a pressure gradient.[23] Because Stern conductance can only act to reduce the efficiency as it provides an additional pathway for power

dissipation, the predicted efficiencies in this paper may be regarded as upper limits. Indeed, recent experiments on the energy conversion efficiency in rectangular silica nanochannels, which we will present elsewhere,[24] reveal a reduction in efficiency due to the presence of a Stern conductance, although they confirm other predictions by this paper such as the peak in efficiency at low salt. It is not known whether Stern conductance is a general feature of all materials, but it is clearly an important material parameter to consider when designing nanochannels for optimal efficiency.

Electrical Output Power of a Macroscopic Device. We now calculate the electrical power that could in principle be obtained from a compact (hand-held) electrokinetic energy conversion device. The hypothetical device consists of a 1-mm-thick, 10×10 cm^2 glass filter that consists of an array of parallel rectangular, slitlike nanochannels. The output power is proportional to the area of this filter, as it scales linearly with the number of parallel channels and the channel width. The height of each nanochannel is 500 nm, small enough for strong double-layer overlap at low salt ($\kappa h \ll 1$) and the channel surface charge is optimized for maximum energy conversion efficiency ($h/2\lambda \cong 8$). The filter porosity, the fraction of the filter area available for fluid flow, is taken to be 50%. For an applied pressure $\Delta p = 5$ bar, the output power of this device is calculated to be 2.6 W for Li^+ as the counterion in aqueous solution.

Conclusions. On the basis of general considerations, we have shown how a fluidic system's efficiency at converting hydrostatic potential energy to electrical power depends on its linear electrokinetic response properties. Calculations of the electrokinetic properties of slitlike nanochannels based on the Poisson−Boltzmann description of the electrostatics and the Navier−Stokes description of the fluid reveal that the efficiency is maximal at low salt concentrations. In the regime where double layers overlap, co-ions are expelled, and their power-dissipating effects are avoided. In this low-salt limit, the energy conversion efficiency only depends on the product of the fluid viscosity and the counterion mobility and on the ratio of the channel height to the Gouy−Chapman length. A peak in the efficiency at $h/2\lambda \approx 8$ results from opposing effects of the counterion distribution on streaming conductance and ionic conduction, and its magnitude is enhanced with decreasing ion mobility and fluid viscosity. For an aqueous-based system containing Li^+ ions, a maximum energy conversion efficiency of 12% is predicted, as is Watt-level electrical power from a compact device requiring an applied pressure difference of 5 bar.

Acknowledgment. We acknowledge discussions with Serge Lemay and funding from NWO, FOM, and NanoNed.

References

(1) Osterle, J. F. *J. Appl. Mech.* **1964**, *31*, 161.
(2) Yang, J.; Lu, F.; Kostiuk, L. W.; Kwok, D. Y. *J. Micromech. Microeng.* **2003**, *13*, 963.
(3) Olthuis, W.; Schippers, B.; Eijkel, J.; van den Berg, A. *Sens. Actuators, B* **2005**, *111*, 385.
(4) Chun, M.-S.; Lee, T. S.; Choi, N. W. *J. Micromech. Eng.* **2005**, *15*, 710.
(5) Daiguji, H.; Yang, P.; Szeri, A. J.; Majumdar, A. *Nano Lett.* **2004**, *4*, 2315.
(6) van der Heyden, F. H. J.; Stein, D.; Dekker, C. *Phys. Rev. Lett.* **2005**, *95*, 116104.
(7) Stein, D.; Kruithof, M.; Dekker, C. *Phys. Rev. Lett.* **2004**, *93*, 035901.
(8) van der Heyden, F. H. J.; Stein, D.; Besteman, K.; Lemay, S. G.; Dekker, C. *Phys. Rev. Lett.* **2006**, *96*, 224502.
(9) Brunet, E.; Ajdari, A. *Phys. Rev. E* **2004**, *69*, 016306.
(10) Mazur, P.; Overbeek, J. T. G. *Recl. Trav. Chim.* **1951**, *70*, 83.
(11) Saxen, U. *Wied. Ann.* **1892**, *47*, 46.
(12) (a) Chen, C.−H.; Santiago, J. G. *J. Micromech. Microeng.* **2002**, *11*, 672. (b) Yao, S.; Santiago, J. G. *J. Colloid Interface Sci.* **2003**, *268*, 133 and 143. (c) Wang, P.; Chen, Z.; Chang, H.-C. *Sens. Actuators, B* **2006**, *113*, 500.
(13) Min, J. Y.; Hasselbrink, E. F.; Kim, S. J. *Sens. Actuators, B* **2004**, *98*, 368.
(14) Werner, C.; Körber, H.; Zimmermann, R.; Dukhin, S.; Jacobasch, H.-J. *J. Colloid Interface Sci.* **1998**, *208*, 329.
(15) Behrens, S. H.; Grier, D. G. *J. Chem. Phys.* **2001**, *115*, 6716.
(16) Verwey, E.; Overbeek, J. *Theory of the Stability of Liophobic Colloids*; Elsevier: New York, 1948.
(17) (a) Israelachvili, J.; Wennerström, H. *Nature* **1996**, *379*, 219. (b) Zhu, Y.; Granick, S. *Phys. Rev. Lett.* **2001**, *87*, 096104.
(18) We used viscosity $\eta_w = 0.93$ mPas and relative permittivity $\epsilon = 79$ for water, and temperature $T = 296.15$ K. The ion mobilities $\mu_{K^+} = 7.32$, $\mu_{Li^+} = 3.86$, $\mu_{H^+} = 34.8$, $\mu_{Na^+} = 4.99$ and $\mu_{Cl^-} = -7.60 \times 10^{-8}$ m^2/Vs were obtained from their limiting equivalent conductivities (Coury, L. *Curr. Sep.* **1999**, *18*, 3.), and $\mu_{TAmA^+}/\mu_{K^+} = 0.237$ is taken from Barry, P. H.; Lynch, J. W. *J. Membr. Biol.* **1991**, *121*, 101.
(19) Andelman, D. *Proc. NATO Adv. Study Inst. & SUSSP on "Soft Condensed Matter Physics in Molecular and Cell Biology"*, **2005**.
(20) Unlike the efficiency, the output power exhibits a different scaling for η and μ, as the input power rougly scales with $1/\eta$ and is independent of μ. Reducing the viscosity therefore increases the output power much more compared to reducing μ.
(21) The relation $\varepsilon_{max} \propto R_{ch}S_{str}^2$ is accurate for the range of efficiencies in Figure 4. The linear response of ε_{max} (eq 16) in the limit $h/2\lambda \rightarrow 0$ is found to be $\varepsilon_{max} \simeq (1/2)(2\epsilon\epsilon_0 kT/\mu\eta e)(h/2\lambda) = h|\sigma|/24\mu\eta$.
(22) The terms in the sum in eq 18 represent the convective and conductive contributions to the electrically driven ion transport with a ratio of $1:\mu\eta e/2\epsilon\epsilon_0 kT$. The dimensionless parameter $\mu\eta e/2\epsilon\epsilon_0 kT$ thus represents the relative importance of the ionic conduction compared to the electro-osmotic ion transport.[7] Minimizing this parameter improves the efficiency (inset of Figure 4).
(23) Lyklema, J. *J. Phys.: Condens. Matter* **2001**, *13*, 5027.
(24) van der Heyden, F. H. J.; Bonthuis, D. J.; Stein, D.; Meyer, C.; Dekker, C. to be submitted for publication.

NL061524L